Open cycle traveling wave thermoacoustics: Mean temperature difference at the regenerator interface

Nathan T. Weiland[a)]
School of Mechanical Engineering, Georgia Institute of Technology, Atlanta, Georgia 30332

Ben T. Zinn
School of Aerospace Engineering, Georgia Institute of Technology, Atlanta, Georgia 30332

(Received 18 April 2003; revised 10 August 2003; accepted 8 September 2003)

In an open cycle traveling wave thermoacoustic engine, the hot heat exchanger is replaced by a steady flow of hot gas into the regenerator to provide the thermal energy input to the engine. The steady-state operation of such a device requires that a potentially large mean temperature difference exist between the incoming gas and the solid material at the regenerator's hot side, due in part to isentropic gas oscillations in the open space adjacent to the regenerator. The magnitude of this temperature difference will have a significant effect on the efficiencies of these open cycle devices. To help assess the feasibility of such thermoacoustic engines, a numerical model is developed that predicts the dependence of the mean temperature difference upon the important design and operating parameters of the open cycle thermoacoustic engine, including the acoustic pressure, mean mass flow rate, acoustic phase angles, and conductive heat loss. Using this model, it is also shown that the temperature difference at the regenerator interface is approximately proportional to the sum of the acoustic power output and the conductive heat loss at this location. [DOI: 10.1121/1.1621859]

PACS numbers: 43.35.Ud, 44.27.+g [RR] Pages: 2791–2798

I. INTRODUCTION

Research in thermoacoustics has been limited mostly to closed cycle designs in recent years, though there is a potential for significant improvements in efficiency by using open cycle thermoacoustic devices. In such systems, a slow mean flow is superimposed on the acoustic field in order to replace one of the heat exchangers with a convective heat transfer process.[1,2] This requires, however, that the mean flow velocity be an order of magnitude smaller than the acoustic velocity in order to keep thermal convection effects from overwhelming the thermoacoustic effects in the device. In most cases, an additional thermodynamic benefit is gained in that the open cycle thermoacoustic process is very efficient in converting the thermal energy in the convected fluid into acoustic energy, or vice versa. This was the major impetus for the construction and testing of the first open cycle thermoacoustic device, Los Alamos's standing wave refrigerator,[1–3] which cools a stream of gas as it passes through the stack. Greater commercial potential exists, however, for open cycle traveling wave thermoacoustic devices, as they possess an efficiency advantage over their inherently irreversible standing wave counterparts.[4] For instance, in the natural gas liquefier being developed jointly by Los Alamos National Lab and Praxair Inc.,[5] the natural gas that is burned to power the liquefier could be routed directly through the thermoacoustic engine in an open cycle configuration, thereby eliminating the hot heat exchanger and providing a simpler and possibly more efficient means of converting fuel energy into acoustic energy.

A diagram of a basic open cycle traveling wave thermoacoustic engine is shown in Fig. 1, where the slow mean flow of hot gas approaches the regenerator from the right. Heat is removed at the cold heat exchanger on the left side of the regenerator, setting up a temperature gradient through which an acoustic traveling wave is amplified in passing from the cold end of the regenerator to the hot end. However, as will be shown in the following, the joining conditions at the interface between the regenerator and the adjacent open duct require that a substantial mean temperature difference exist between the incoming mean flow and the regenerator's solid material. Since this may have profound effects on the acoustics, thermodynamics, and efficiency of the open cycle thermoacoustic engine, the remainder of this study will focus on developing a model that can be used to predict the magnitude of this temperature difference.

The physical processes responsible for creating the temperature difference at the regenerator/open duct interface are shown schematically for various gas parcels in Fig. 2, which can be viewed as a magnification of the control volume surrounding the regenerator interface in Fig. 1. Gas parcels that start the acoustic cycle at various locations within the regenerator are shown in Figs. 2(a)–(d). For good gas–solid thermal contact within the regenerator, these parcels of gas remain at the regenerator's temperature until they enter the open duct, where they undergo isentropic temperature oscillations in concert with the pressure oscillations of the traveling acoustic wave. These oscillations cause the gas parcels to re-enter the regenerator at temperatures below that of the regenerator,[6] where they receive heat from the regenerator solid and are rapidly heated back up to the temperature of the regenerator at the interface, T_{re}. At the end of the acoustic cycle, fresh gas parcels enter the regenerator for the first time due to the steady mean flow of gas toward the regenerator, as

a)Electronic mail: gte852f@mail.gatech.edu

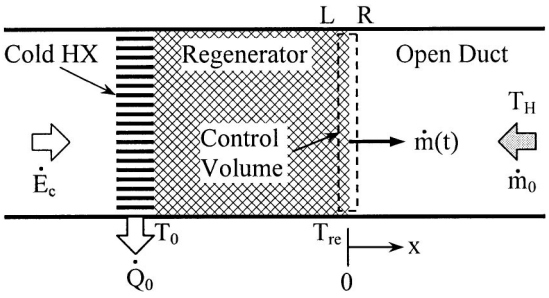

FIG. 1. A schematic of a basic open cycle traveling wave thermoacoustic engine. A steady flow of gas with mean temperature T_H flows into the regenerator, whose hot end is at the temperature T_{re}. A cold heat exchanger rejects heat to ambient temperature at the other end of the regenerator, and the resulting temperature gradient in the regenerator is used to amplify the acoustic traveling wave entering its cold end. An analysis of the control volume, which includes the interface between the regenerator and the open duct, is used to determine the difference between the temperatures T_H and T_{re}. State properties on the left and right of the control volume are labeled with subscripts "*L*" and "*R*," respectively.

depicted in Figs. 2(e) and (f). These gas parcels isentropically oscillate about their mean temperature, T_H, until they enter the regenerator, at which time they are cooled to T_{re} by contact with the regenerator's solid material. In the absence of other sources of heat input or output, a heat balance of the regenerator solid at the interface shows that the heat transferred from the solid to the cold returning gas must equal the heat transferred from the fresh gas to the regenerator solid, if the solid material is to maintain a constant mean temperature during steady-state operation. Satisfying this criterion gives rise to the mean temperature difference between the regenerator solid and the hot incoming gas, as cited earlier.

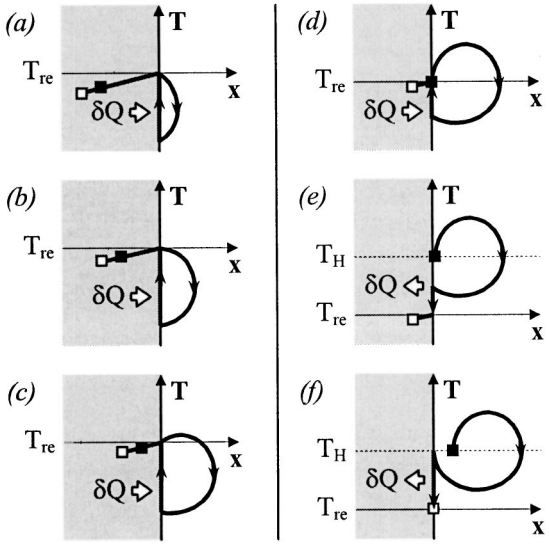

FIG. 2. A schematic of the temperature and acoustic displacement histories of various gas parcels near the regenerator/open duct interface, over the course of an acoustic cycle. The closed squares denote the starting position of each parcel, and the open squares denote the final position. The net displacement between the starting and finishing positions is due to the mean mass flux. Gas parcels in (a)–(d) start their motion inside the regenerator, undergo isentropic temperature oscillations outside the regenerator that reduce their temperatures, and are heated to the regenerator's temperature, T_{re}, upon re-entry. Gas parcels in (e) and (f) start their motions outside the regenerator, oscillate isentropically about the mean temperature, T_H, and cool down to T_{re} upon entering the regenerator at the end of the acoustic cycle.

The effect of a temperature difference within or between thermoacoustic components has been a subject of several studies in thermoacoustics. This topic was first broached by Swift,[7] who pointed out that for net solid–gas heat transfer to occur within a heat exchanger, a difference must exist between the solid temperature and the spatially and temporally averaged gas temperature within the heat exchanger. Brewster *et al.*[8] extended this concept to include the heat transfer between a thermoacoustic stack and its heat exchangers, though their analysis was limited only to standing wave thermoacoustic devices. Research that is more closely related to the problem at hand was first performed by Smith and Romm[6] for component interface losses in Stirling engines, and later on by Kittel[9] and Bauwens[10] for similar interface losses in pulse tube refrigerators. Swift[11] subsequently applied these concepts to the general field of thermoacoustics, and has developed relationships that are frequently used to estimate losses and joining conditions between components in thermoacoustic devices. However, none of these studies consider the effects of mean flow on the component interface dynamics, thus the development of a new theoretical framework is required for studying the component interface conditions in open cycle thermoacoustic devices.

It should also be noted that while this study deals primarily with open cycle, traveling wave thermoacoustic engines, the problem of determining the temperature difference at the regenerator/open duct interface is also of concern in thermoacoustic refrigerators and heat pumps of the same type, as this temperature difference critically impacts the efficiencies of all of these devices. However, this paper effectively demonstrates the procedure involved in the determination of this temperature difference by focusing solely on the traveling wave engine application.

II. MASS FLUX MODEL

The formulation used to model the open cycle thermoacoustic engine follows the formulation developed by Smith and Romm,[6] with some modifications to account for the presence of mean flow. The model considers conditions within a control volume that encloses the hot side interface of the regenerator, as shown in Fig. 1. The control volume's left and right boundaries, designated with the subscripts *L* and *R*, are located inside the solid matrix of the regenerator and in the adjoining open duct, respectively, and are close enough together that the control volume can be assumed to contain a negligible amount of mass. To simplify the analysis, it is assumed that the flow is one-dimensional, and that there is no axial conduction or mixing between the parcels of gas that move axially in and out of the control volume.

A. Mass flux

To begin, the mass flux passing through the control volume is assumed to be given by

$$\dot{m}(t) = \dot{m}_0 + \dot{m}_1 \sin(\omega t + \phi), \tag{1}$$

where $\dot{m}_0$ and $\dot{m}_1$ are the magnitudes of the mean and oscillating components of the mass flux, respectively, ω is the angular frequency of the acoustic oscillations, and ϕ is a

phase shift used to set a reference time below. Having assumed that the control volume contains a negligible amount of mass, it can be further assumed that the mass fluxes crossing the left and right sides of the control volume are equal (i.e., $\dot{m}_L = \dot{m}_R$).

It is convenient to nondimensionalize the model equations in order to eliminate the dependence on the angular frequency. Introducing a dimensionless time, $\hat{t} \equiv \omega t$, and dimensionless mass fluxes, $\hat{m} \equiv \dot{m}/\dot{m}_1$ and $\hat{m}_0 \equiv \dot{m}_0/\dot{m}_1$, Eq. (1) can be rewritten as

$$\hat{m}(\hat{t}) = \hat{m}_0 + \sin(\hat{t} + \phi). \tag{2}$$

Note that nondimensionalizing the mass fluxes by $\dot{m}_1$ instead of $\dot{m}_0$ is more practical for consideration of the limiting case in which there is no mean mass flux.

By choosing to let $\hat{m} = 0$ at $\hat{t} = 0$, the phase shift becomes

$$\phi = \sin^{-1}(-\hat{m}_0). \tag{3}$$

Here, Eq. (3) specifies that $|\hat{m}_0| \leqslant 1$, though for practical purposes, we require $|\hat{m}_0| \leqslant 0.1$ to satisfy the condition that the mean velocity be an order of magnitude smaller than the oscillating velocity in an open cycle thermoacoustic device.[2] Further, this study will only consider the processes that occur during one acoustic cycle, i.e., $0 \leqslant \hat{t} \leqslant 2\pi$, where $\hat{m} = 0$ at $\hat{t} = 0$ and $\hat{t} = 2\pi$, according to Eqs. (2) and (3).

An important parameter in this study is the time, $\hat{t}_{\text{mid}}$, at which the gas ceases to flow out of the regenerator, reverses direction, and begins to flow back into the regenerator. Noting that $\hat{m}(\hat{t}_{\text{mid}}) = 0$, that $\hat{t}_{\text{mid}}$ should be close to π in value, and that the sine function has odd symmetry about π, Eqs. (2) and (3) can be used to show that

$$\hat{t}_{\text{mid}} = \pi - 2\phi. \tag{4}$$

B. Total mass

In later sections, it will be necessary to relate the time at which a particular gas parcel leaves the regenerator to the time at which it re-enters the regenerator. This is accomplished by tracking the total mass, m, that has passed from the regenerator to the open duct during the acoustic cycle. Integrating Eq. (1) and nondimensionalizing yields

$$\hat{m}(\hat{t}) = \hat{m}_0 \hat{t} - \cos(\hat{t} + \phi) + \cos(\phi), \tag{5}$$

where the total dimensionless mass has been defined as $\hat{m} \equiv m\omega/\dot{m}_1$.

The mass flux and total mass displacement, as described by Eqs. (2) and (5), are plotted in Fig. 3, where three distinct time periods within the acoustic cycle can be identified. The first, denoted by the subscript "*a*," describes the time period $0 \leqslant \hat{t}_a \leqslant \hat{t}_{\text{mid}}$ when the gas is flowing from left to right out of the regenerator. At the time $\hat{t}_{\text{mid}}$, the gas reverses direction and starts flowing back to the left, thus the total mass that has entered the open duct since the start of the acoustic cycle, $\hat{m}$, is a maximum at this time. The second time period is defined as the time during which gas parcels that left the regenerator return to the regenerator. Since a stratified flow has been assumed, the time at which a representative gas parcel leaves the regenerator, $\hat{t}_a$, can be related to the time at which the same parcel re-enters the regenerator, $\hat{t}_b$, by equating the total mass displacement at these times as shown in Fig. 3, i.e., $\hat{m}(\hat{t}_a) = \hat{m}(\hat{t}_b)$. Using Eq. (5), $\hat{t}_b$ can thus be related to $\hat{t}_a$ by solving

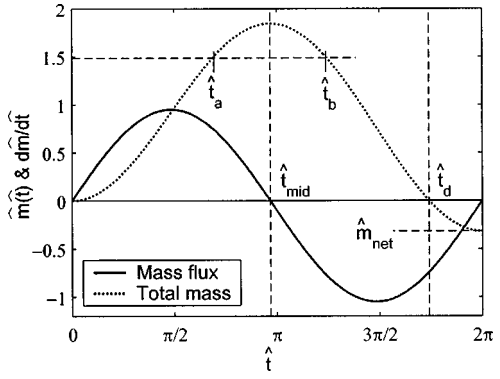

FIG. 3. Time dependence of the dimensionless mass flux and total mass displacement during an acoustic cycle in which $\hat{m}_0 = -0.05$. Three distinct time periods are identified by the dashed vertical lines. In the first time period, gas flows to the right, leaving the regenerator, until it comes to a stop at time $\hat{t}_{\text{mid}}$. In the second time period, that same gas flows back to the left, returning to the regenerator. The time at which a particular gas parcel re-enters the regenerator, $\hat{t}_b$, is linked to the time at which it leaves the regenerator, $\hat{t}_a$, by the total mass displacement. In the third time period, after all of the original gas has returned to the regenerator at time $\hat{t}_d$, fresh gas flows into the regenerator until the end of the acoustic cycle. The net mass displacement for the acoustic cycle, $\hat{m}_{\text{net}}$, is also shown.

$$\hat{m}_0 \hat{t}_a - \cos(\hat{t}_a + \phi) = \hat{m}_0 \hat{t}_b - \cos(\hat{t}_b + \phi), \tag{6}$$

where $\hat{t}_b$ falls between $\hat{t}_{\text{mid}}$ and a time $\hat{t}_d$, which marks the start of the third time period.

In the stratified flow assumption, two parcels of gas that start the acoustic cycle adjacent to each other, one inside the regenerator and one outside, can have vastly different states, thus the regenerator interface experiences a discontinuity in gas properties as the gas in the open duct flows from right to left through the control volume at time $\hat{t}_d$, the "discontinuity" time. This time corresponds to the time at which $\hat{m} = 0$ again, and can be found by solving

$$\hat{m}(\hat{t}_d) = \hat{m}_0 \hat{t}_d - \cos(\hat{t}_d + \phi) + \cos(\phi) = 0 \tag{7}$$

for $\hat{t}_d$, where $\hat{t}_{\text{mid}} < \hat{t}_d < 2\pi$. This time marks the beginning of the third time period, denoted by the subscript "*c*," $\hat{t}_d \leqslant \hat{t}_c \leqslant 2\pi$, during which fresh gas parcels enter the regenerator for the first time due to the presence of a mean flow. At the end of the acoustic cycle, a net mass of

$$\hat{m}(\hat{t} = 2\pi) \equiv \hat{m}_{\text{net}} = 2\pi\hat{m}_0 \tag{8}$$

has been transported into the regenerator as a result of the mean mass flux as depicted in Fig. 3.

III. THERMODYNAMIC MODEL

Next, the thermodynamic properties of the gas need to be determined on each side of the control volume for all times during the acoustic cycle. To facilitate this analysis, it is assumed that the pressure in the control volume does not depend on axial location, and is given by

$$\hat{p}(\hat{t}) = 1 + \hat{p}_1 \sin(\hat{t} + \phi + \theta), \tag{9}$$

where $\hat{p} \equiv p/p_0$ and $\hat{p}_1 \equiv p_1/p_0$. Here, p_0 is the mean pressure, p_1 is the amplitude of the acoustic pressure, and θ is the phase angle by which the acoustic pressure leads the acoustic mass flux, where attention is restricted to $-\pi/2 < \theta < \pi/2$ in this work, since acoustic energy flux is positive according to the sign conventions of this study.

A. Gas temperatures

The temperature and position histories of various gas parcels near the regenerator interface are shown schematically in Fig. 2 above, although it is not necessary to calculate these histories, as the only temperatures of interest in this study are those of the gas parcels as they enter and leave the control volume. To simplify matters, it is assumed that the gas properties can be related by the ideal gas equation of state, and that there is perfect thermal contact between the gas and the solid within the regenerator (i.e., $T_L = T_{\mathrm{re}}$ for all $\hat{t}$). Since accounting for the transient heating effects in the regenerator would require a finite-width control volume, thermal conductivity and specific heat properties of the gas, and details on the regenerator's internal geometry, neglecting these effects greatly simplifies the model at the expense of a slightly diminished accuracy.

During the first time period, gas exits the regenerator at temperature T_{re} and crosses the right-hand boundary of the control volume, so $T_{R,a} = T_{\mathrm{re}}$. Upon exiting the regenerator, gas parcels undergo isentropic temperature oscillations as a result of the acoustic pressure oscillations in the open duct to the right of the regenerator, as depicted in Figs. 2(a)–(d). For an isentropic process in an ideal gas, the pressure and temperature are related by

$$\frac{T}{T_{\mathrm{ref}}} = \left(\frac{p}{p_{\mathrm{ref}}} \right)^{(\gamma-1)/\gamma}, \tag{10}$$

where γ is the ratio of specific heats. The reference conditions for a particular parcel of gas correspond to the temperature and pressure of the gas when it first encounters the isentropic environment upon exiting the regenerator at time $\hat{t}_a$. The time at which this gas parcel returns to the regenerator is determined by solving Eq. (6) for $\hat{t}_b$, and the dimensionless temperature of the gas parcel at this time, $\hat{T}_{R,b}$, is then found from Eq. (10):

$$\hat{T}_{R,b} = \left[\frac{1 + \hat{p}_1 \sin(\hat{t}_b + \phi + \theta)}{1 + \hat{p}_1 \sin(\hat{t}_a + \phi + \theta)} \right]^{(\gamma-1)/\gamma}, \tag{11}$$

where the temperature has been nondimensionalized with respect to the regenerator temperature (i.e., $\hat{T} \equiv T/T_{\mathrm{re}}$).

The temperature of the incoming gas during the third time period can be similarly obtained, though the reference states for temperature and pressure must be redefined. In the open duct, the gas temperature isentropically oscillates about a mean temperature, T_H, as a result of the pressure oscillations, as depicted in Figs. 2(e) and (f). In the course of these oscillations, $T = T_H$ when $p = p_0$, so taking T_H and p_0 as the reference states in Eq. (10) for the gas parcels that begin the acoustic cycle inside the open duct, the temperature at the time the gas parcels first enter the regenerator, $\hat{T}_{R,c}$, can be expressed as

$$\hat{T}_{R,c} = \hat{T}_H [1 + \hat{p}_1 \sin(\hat{t}_c + \phi + \theta)]^{(\gamma-1)/\gamma}. \tag{12}$$

B. Thermal energy balance

Having determined the temperature of the gas crossing each of the control volume's boundaries, the heat balance within the control volume can now be examined. Assuming that kinetic energy and viscous effects are negligible, a quasi-one-dimensional energy equation can be written as

$$\frac{\partial(\rho e)}{\partial t} + \frac{\partial(\rho u h)}{\partial x} + \nabla \cdot \mathbf{q} = 0, \tag{13}$$

where ρ is the gas density, e is the internal energy, u is the gas velocity in the x direction, h is the enthalpy, and $\mathbf{q}$ is the heat flux vector. Using the ideal gas law and the state relationships $e = h - p/\rho$ and $dh = c_p dT$, the first term in Eq. (13) can be written as: $\partial(\rho e)/\partial t = (\partial p/\partial t)/(\gamma - 1)$.

Integrating over the control volume then yields

$$\frac{V}{\gamma - 1} \frac{dp}{dt} + [\dot{m} h]_R - [\dot{m} h]_L + \int \nabla \cdot \mathbf{q} \, dV = 0. \tag{14}$$

Assuming that the periphery of the device is well-insulated, the heat flux vector, $\mathbf{q}$, consists of two primary components, axial heat conduction and lateral heat transfer between the gas and the regenerator's solid material. Using the divergence theorem and Fourier's law for the conductive heat flux yields

$$\frac{V}{\gamma - 1} \frac{dp}{dt} + \left[\dot{m} h - Ak \frac{dT}{dx} \right]_R - \left[\dot{m} h - Ak \frac{dT}{dx} \right]_L = \dot{Q}, \tag{15}$$

where A is the cross-sectional area occupied by the gas, k is the thermal conductivity of the gas, and $\dot{Q}$ is generically defined as the heat transfer rate between the regenerator solid and the gas in the control volume, where heat transfer to the gas is positive. This equation can be further simplified by applying the above assumption of an infinitely thin control volume, which eliminates the first term on the left-hand side of Eq. (15). Finally, if thermal conduction effects in the gas are assumed to be negligible, Eq. (15) can be written nondimensionally as

$$\hat{Q} = \hat{m}(\hat{T}_R - 1), \tag{16}$$

where the dimensionless heat flux is defined as $\hat{Q} \equiv \dot{Q}/\dot{m}_1 c_p T_{\mathrm{re}}$.

Although thermal conduction in the gas has been neglected, conduction in the solid of the regenerator may still be important, as the thermal conductivities of solids are generally orders of magnitude larger than those for gases, and the solid material constitutes a significant volume fraction of the regenerator. To account for this conductive heat flux, a thermal energy balance of the regenerator solid is required. Assuming that heat transfer to the gas and conduction through the left side of the control volume are the only heat fluxes in or out of the solid, this energy balance can be written nondimensionally as

$$\frac{d\hat{E}_s}{d\hat{t}} = \hat{Q}_k - \hat{Q}, \tag{17}$$

where $\hat{E}_s \equiv \omega E_s / \dot{m}_1 c_p T_{re}$, in which E_s is the thermal energy of the solid in the control volume, and $\hat{Q}_k \equiv -A_s k_s (dT/dx)_{int} / \dot{m}_1 c_p T_{re}$, where A_s is the cross-sectional area of the solid, k_s is the thermal conductivity of the solid, and $(dT/dx)_{int}$ is temperature gradient of the solid at the regenerator interface.

In steady state operation, the solid material of the regenerator maintains a constant temperature, T_{re}, thus there must be no net energy change in the solid material of the regenerator over the course of an acoustic cycle, i.e.,

$$\int_0^{2\pi} \frac{d\hat{E}_s}{d\hat{t}} d\hat{t} = \int_0^{2\pi} \hat{Q}_k d\hat{t} - \int_{\hat{t}_{mid}}^{\hat{t}_d} \hat{Q}_b d\hat{t}_b - \int_{\hat{t}_d}^{2\pi} \hat{Q}_c d\hat{t}_c = 0. \tag{18}$$

In this expression, the gas–solid heat transfer integral has been split into its contributions from the second and third time periods, $\hat{Q}_b$ and $\hat{Q}_c$, respectively, while the contribution from the first time period has been neglected since no heat is transferred between the gas and the regenerator solid during this time. Substituting Eqs. (11) and (12) for $\hat{T}_{R,b}$ and $\hat{T}_{R,c}$, respectively, into Eq. (16), expressions for the heat fluxes during the second and third time periods are obtained:

$$\hat{Q}_b(\hat{t}_b) = \hat{m}(\hat{t}_b) \left(\left[\frac{\hat{p}(\hat{t}_b)}{\hat{p}(\hat{t}_a)} \right]^{(\gamma-1)/\gamma} - 1 \right), \tag{19}$$

$$\hat{Q}_c(\hat{t}_c) = \hat{m}(\hat{t}_c) (\hat{T}_H [\hat{p}(\hat{t}_c)]^{(\gamma-1)/\gamma} - 1). \tag{20}$$

In each of these equations, the mass fluxes and pressures are given (for the appropriate times) by Eqs. (2) and (9), respectively, and $\hat{t}_a$ in Eq. (19) is related to $\hat{t}_b$ by Eq. (6).

IV. THE TEMPERATURE DIFFERENCE

Substituting Eqs. (19) and (20) into the heat balance of Eq. (18) yields, after some manipulation, an equation for the ratio of the mean temperature of the incoming gas to the temperature of the regenerator solid:

$$\hat{T}_H = \frac{\int_{\hat{t}_d}^{2\pi} \hat{m} d\hat{t}_c + \int_{\hat{t}_{mid}}^{\hat{t}_d} \hat{m} \left(1 - \left[\frac{\hat{p}(\hat{t}_b)}{\hat{p}(\hat{t}_a)} \right]^{(\gamma-1)/\gamma} \right) d\hat{t}_b + 2\pi \hat{Q}_k}{\int_{\hat{t}_d}^{2\pi} \hat{m} [\hat{p}(\hat{t}_c)]^{(\gamma-1)/\gamma} d\hat{t}_c}. \tag{21}$$

The integrations in Eq. (21) are performed numerically on a PC to determine the value of $\hat{T}_H$ that satisfies the heat balance. In an actual open cycle thermoacoustic engine, the mean flow gas temperature would be a known, fixed quantity, and the steady-state heat balance of Eq. (18) would be solved to determine the temperature at the hot face of the regenerator. Regardless, Eq. (21) solves for the ratio between the two temperatures, so knowing one temperature allows for the solution of the other temperature.

A plot of the calculated time history of the temperature at the right-hand side of the control volume is shown for representative choices of independent parameters in Fig. 4(a). The right-side temperature, T_R, is equal to the regenerator temperature during the first time period, and is lower than the regenerator temperature during the second time period. This is consistent with the results of Smith and Romm,[6] who have shown that if work is generated by the engine (i.e., $-\pi/2 < \theta < \pi/2$), then the isentropic oscillations outside the regenerator cause the gas to re-enter the regenerator at lower temperatures. At the end of the second time period, $\hat{t}_d$, a discontinuity in temperature occurs as the fresh, hotter gas enters the regenerator for the first time. The plot of the gas–solid heat transfer rate versus time in Fig. 4(b) shows the added effect of the mass flux, and illustrates the heat balance described in Eq. (18), where the area under the curves during the second and third time periods must equal one another in the absence of a conductive heat flux. The various curves in Figs. 4(a) and (b) show the effects of varying mean mass flow rates on the temperature and heat flux histories, which will be discussed further in a later section.

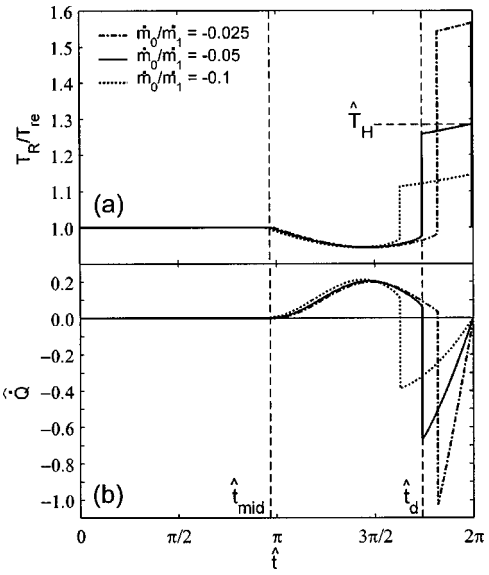

FIG. 4. Time dependence of (a) the dimensionless temperature on the right side of the control volume and (b) the dimensionless heat flux from the regenerator solid, during an acoustic cycle for the conditions: $\hat{p}_1 = 0.1$, $\gamma = 1.4$, $\theta = 0$, and $\hat{Q}_k = 0$. The mean incoming gas temperature and relevant time periods are marked for $\hat{m}_0 = -0.05$ (solid line), which correspond to the same time periods shown in Fig. 3. For comparison, the temperature and heat flux histories for $\hat{m}_0 = -0.025$ and $\hat{m}_0 = -0.1$ are also shown.

A. Temperature difference approximation

Predicting the mean temperature difference with Eq. (21) is fairly cumbersome, and is not very practical for quick design calculations. Several approximations can be made to this equation to yield a simpler expression that reasonably estimates the temperature difference, $\hat{T}_H$, and provides a clearer understanding of how it is affected by various independent parameters. First, by expanding the pressure term in the denominator of Eq. (21) in a binomial series and assuming that the acoustic pressure amplitude is much smaller than the mean pressure (i.e., $\hat{p}_1 \ll 1$), the denominator of Eq. (21) can be approximated by

$$\int_{\hat{t}_d}^{2\pi} \hat{m} [\hat{p}(\hat{t}_c)]^{(\gamma-1)/\gamma} d\hat{t}_c \approx \int_{\hat{t}_d}^{2\pi} \hat{m} d\hat{t}_c = 2\pi \hat{m}_0, \tag{22}$$

where the last integral is equal to the net mass displacement for the entire acoustic cycle (see Fig. 3). Substitution of Eq. (22) into Eq. (21) for the temperature difference yields

$$\hat{T}_H \approx 1 + \frac{1}{2\pi \hat{m}_0} \int_{\hat{t}_{\text{mid}}}^{\hat{t}_d} \hat{m} \left(1 - \left[\frac{\hat{p}(\hat{t}_b)}{\hat{p}(\hat{t}_a)} \right]^{(\gamma-1)/\gamma} \right) d\hat{t}_b + \frac{\hat{Q}_k}{\hat{m}_0}, \tag{23}$$

where Eq. (22) has also been applied to the first term in the numerator of Eq. (21).

To simplify the pressure term within the integral in Eq. (23), the pressure ratio can be expanded in a Taylor series with the use of Eq. (9), and the resulting expression can be further expanded in a binomial series to account for the pressure ratio's exponent. Extracting the θ dependence from this result and using Eq. (6) yields

$$\begin{aligned} 1 - \left[\frac{\hat{p}(\hat{t}_b)}{\hat{p}(\hat{t}_a)} \right]^{(\gamma-1)/\gamma} \approx{}& \frac{\gamma-1}{\gamma} \hat{p}_1 \hat{m}_0 (\hat{t}_a - \hat{t}_b) \sin\theta \\ &+ \frac{\gamma-1}{\gamma} \hat{p}_1 \cos\theta [\sin(\hat{t}_a + \phi) \\ &- \sin(\hat{t}_b + \phi)], \end{aligned} \tag{24}$$

where all terms that are second order and higher in the acoustic pressure amplitude have been neglected. This expression can be further simplified by assuming that the mean mass flux is much smaller than the acoustic mass flux, i.e., $\hat{m}_0 \ll 1$, which eliminates the first term on the right-hand side of Eq. (24). Substituting Eqs. (2) and (24) into Eq. (23) and eliminating terms of the order of $\hat{m}_0$ from the integral yields

$$\begin{aligned} \hat{T}_H \approx{}& 1 + \frac{\hat{Q}_k}{\hat{m}_0} + \frac{\gamma-1}{\gamma} \frac{\hat{p}_1 \cos\theta}{2\pi \hat{m}_0} \int_{\hat{t}_{\text{mid}}}^{\hat{t}_d} \sin(\hat{t}_b + \phi) \\ &\times [\sin(\hat{t}_a + \phi) - \sin(\hat{t}_b + \phi)] d\hat{t}_b, \end{aligned} \tag{25}$$

where the integral now contains only variables that are a function of $\hat{m}_0$. In the limiting case in which $\hat{m}_0$ approaches zero, it can be shown that: $\phi \to 0$, $\hat{t}_a \to 2\pi - \hat{t}_b$, $\hat{t}_{\text{mid}} \to \pi$, and $\hat{t}_d \to 2\pi$.

Using these limits to evaluate the integral in Eq. (25) yields a compact expression for the estimated temperature difference:

$$\hat{T}_H \approx 1 - \frac{\gamma-1}{\gamma} \frac{\hat{p}_1 \cos\theta}{2\hat{m}_0} + \frac{\hat{Q}_k}{\hat{m}_0}. \tag{26}$$

Note that in this estimate, $\hat{T}_H > 1$, since $\hat{m}_0$ and $\hat{Q}_k$ are always negative by the sign conventions used in this study, and $-\pi/2 \leqslant \theta \leqslant \pi/2$.

Given the number of approximations made in arriving at this result, Eq. (26) works remarkably well as an estimate for the true temperature difference given in Eq. (21), with errors of less than 5% for $\hat{p}_1 \leqslant 0.1$, $\gamma \leqslant 1.67$, $-\pi/2 \leqslant \theta \leqslant \pi/2$, $-0.1 \leqslant \hat{m}_0 \leqslant -0.0001$, and $\hat{Q}_k \leqslant 0$. Even for higher acoustic pressure amplitudes (e.g., $\hat{p}_1 \leqslant 0.3$), Eq. (26) approximates the temperature difference to within about 10% of its true value.

To take the estimation of the temperature difference a step further, note that the acoustic energy at the hot side of the regenerator can be approximated by

$$\dot{E}_{re} \approx \frac{p_1 \dot{m}_1 \cos\theta}{2\rho_{\text{re}}}. \tag{27}$$

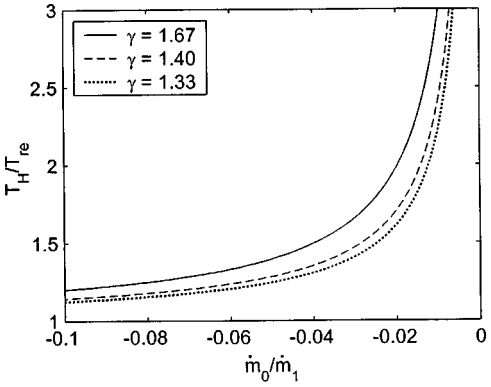

FIG. 5. The dependence of the temperature ratio of the incoming gas and the regenerator solid upon the mean to oscillating mass flux ratio and the ratio of specific heats, γ, for the conditions: $\hat{p}_1 = 0.1$, $\theta = 0$, and $\hat{Q}_k = 0$. Note that the negative mean mass flux indicates gas flow toward the regenerator.

By using Eq. (27), the ideal gas law, and the definitions of the dimensionless variables, Eq. (26) can be rearranged to produce the following interesting result:

$$\dot{m}_0 c_p (T_{\text{re}} - T_H) \approx \dot{E}_{\text{re}} + A_s k_s \left(\frac{dT}{dx} \right)_{\text{int}}. \tag{28}$$

Equation (28) indicates that a substantial temperature difference must exist across the regenerator interface if the engine is going to produce a significant amount of acoustic power. A more broad interpretation of Eq. (28) states that of the thermal energy convected to the regenerator interface at temperature T_H, some of it is convected into the regenerator at temperature T_{re}, some of it is conducted through the regenerator solid, and the remainder is used to create the acoustic energy exiting the regenerator. This acoustic energy is not generated by the processes occurring at the regenerator interface, but rather, this term represents a ''thermoacoustic heat flux'' into the regenerator. Note that in an ideal regenerator of a traveling wave thermoacoustic device, that the acoustic energy flux traveling in one direction is accompanied by a ''thermoacoustic heat flux'' of equal magnitude traveling in the opposite direction.[11] The thermal energy carried by this thermoacoustic ''heat-pumping'' effect, as it is also called, is converted into work in the form of acoustic energy within the regenerator. Therefore, in accordance with Eq. (28), a larger temperature difference at the regenerator interface results in a larger ''thermoacoustic heat flux'' into the regenerator, consequently increasing the acoustic power that is generated with this thermal energy.

B. Effects on the temperature difference

The above-presented analysis shows that the temperature difference between the gas and regenerator depends upon the following five dimensionless parameters: the ratio of mean to oscillating mass fluxes, $\hat{m}_0$, the ratio of acoustic to mean pressures, $\hat{p}_1$, the phase angle by which oscillating pressure leads oscillating mass flux, θ, the ratio of specific heats, γ, and the thermal conduction loss in the regenerator, $\hat{Q}_k$. The parameter with the largest effect on the temperature difference is $\hat{m}_0$, as shown in Fig. 5. As the magnitude of mean mass flux decreases relative to the magnitude of the

acoustic mass flux, $\hat{T}_H$ becomes fairly large. The functional relationship between the temperature difference and the mean mass flux is shown in Eq. (26), where the temperature difference is a function of the inverse of the mean mass flux.

This dependence on the mean mass flux can be explained by considering its effect on the discontinuity time, $\hat{t}_d$, given in Eq. (7). A reduction in $\hat{m}_0$ increases $\hat{t}_d$, thus decreasing the fraction of the acoustic cycle during which the fresh gas enters the regenerator. This effect is depicted in the heat flux plot of Fig. 4(b), where the time at which the discontinuity occurs for $\hat{m}_0=-0.1$ is earlier than the discontinuity time for $\hat{m}_0=-0.05$. As shown in the figure, the total heat transferred to the gas during the second time period (the area under the curve) is only slightly increased by the increased limits of integration. The primary effect of decreasing the mean mass flux and increasing the discontinuity time is to decrease the time allotted for heat transfer from the fresh gas to the regenerator solid. To compensate, the mean temperature of the incoming gas must increase so that the net heat input from the gas (the area under the curve for the third time period) equals that of the heat output from the solid, as expressed in the heat balance in Eq. (18).

As Fig. 5 illustrates, the mean temperature difference between the gas in the regenerator and the open duct is not necessarily small, and can be much larger than the other types of temperature differences noted in the thermoacoustics literature to date.[6–11] This is primarily a result of the mean flow's role as the heat source, whereas other analyses have only investigated temperature differences associated with the use of heat exchangers. Temperature differences of the magnitudes seen here can have a profound effect on the efficiency of the engine, although Eq. (28) would suggest that it may not necessarily be advantageous to minimize this temperature difference, as it is directly linked to the acoustic power output of the engine.

Figure 5 also describes the effect of the ratio of specific heats, γ, on the magnitude of the temperature difference as expressed in Eq. (21). These effects are the result of the influence of γ on the isentropic relationship between temperature and pressure outside the regenerator, as described by Eq. (10). As Eq. (26) shows, the ratio of specific heats has a smaller effect upon the temperature difference than the other independent parameters, however, it is the only one of the five independent parameters that depends upon the gas properties within the engine. As such, monatomic gases ($\gamma\approx1.67$) result in higher temperature differences than nonmonatomic gases. For nonmonatomic gases the mean gas temperature plays a small role, as gaseous combustion products ($T\approx2000\,\mathrm{K}$), for which $\gamma\approx1.33$, will yield slightly lower temperature differences according to Fig. 5, than will ambient-temperature nonmonatomic gases, for which $\gamma\approx1.4$.

The dependence of the temperature difference upon the acoustic phase lag, θ, and the acoustic pressure magnitude, $\hat{p}_1$, is shown in Fig. 6. Consistent with the cos θ dependence predicted in Eq. (26), the acoustic phase shift produces the largest temperature differences near $\theta=0$, corresponding to traveling wave acoustic phasing. This condition maximizes the difference in a gas parcel's temperature from exit to return to the regenerator, which increases $\hat{Q}_b$, the heat flux

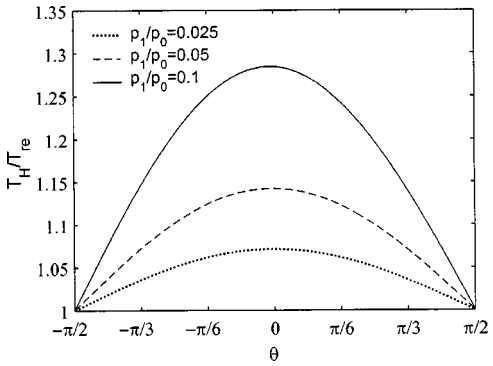

FIG. 6. The dependence of the temperature ratio of the incoming gas and the regenerator solid upon the phase angle by which oscillating pressure leads the oscillating mass flux, θ, and the acoustic to mean pressure ratio, $\hat{p}_1$, for the conditions: $\hat{m}_0=-0.05$, $\gamma=1.4$, and $\hat{Q}_k=0$.

from the regenerator to the incoming gas, and requires that $\hat{Q}_c$ and $\hat{T}_H$ increase correspondingly. The temperature difference decreases away from $\theta=0$, until no temperature difference exists for standing wave acoustic phasing at $\theta=\pm\pi/2$. Since the acoustic displacement, pressure, and temperature are all in phase in a standing wave, a gas parcel will undergo isentropic oscillations outside of the regenerator but will return to the regenerator at the same temperature and pressure as when it left.[11] The addition of mean flow introduces slight phase differences between temperature and displacement over the course of an acoustic cycle, but the resulting heat fluxes cancel one another for $\theta=\pm\pi/2$.

Figure 6 also shows the approximately linear relationship between the acoustic pressure magnitude and the temperature difference of Eq. (21), with higher acoustic pressures resulting in higher temperature differences. This relationship is predicted by Eq. (26) and can be linked to the Taylor series expansion in Eq. (24), where the temperature of the gas returning to the regenerator during the second part of the acoustic cycle, $\hat{T}_{R,b}$, is shown to be approximately proportional to $\hat{p}_1$ for small values of the acoustic pressure magnitude. Therefore, the total heat flux from the solid to the gas during the second part of the acoustic cycle is proportional to $\hat{p}_1$, which is in turn approximately proportional to the temperature difference required to maintain the heat balance. Recognizing the link between the temperature difference and the heat flux across the regenerator's interface, the results in Fig. 6 for both the pressure and phase angle are in qualitative agreement with the results of Smith and Romm.[6]

Finally, Fig. 7 shows the combined effects of the conductive loss term, $\hat{Q}_k$, and the mean mass flux on the temperature difference. While the mean mass flux effect is the same as that shown in Fig. 5, the addition of a conductive heat loss increases the required temperature difference at the regenerator's interface. For a given mean mass flux, this dependence is shown to be approximately linear, as predicted by Eq. (26) for the estimated temperature difference. This behavior is best explained in conjunction with Eq. (18), which states that the total energy change in the regenerator solid over the course of an acoustic cycle is equal to the heat transfer from the gas to the solid during the third time period, minus the heat transferred from the solid to the gas during

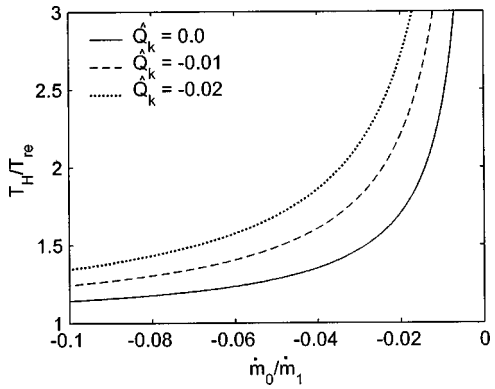

FIG. 7. The dependence of the temperature ratio of the incoming gas and the regenerator solid upon the mean to oscillating mass flux ratio and the dimensionless conductive heat loss, $\hat{Q}_k$, for the conditions: $\hat{p}_1=0.1$, $\theta=0$, and $\gamma=1.4$.

the second time period, minus the heat leaving the control volume via thermal conduction. Therefore, for increasing heat conduction losses, an increasing heat input from the third time period is required (which is proportional to the temperature difference), in order to enforce the condition that there be zero net energy change in the regenerator's solid from one acoustic cycle to the next. As such, minimizing the conductive heat leak increases the portion of the thermal energy input available for conversion to acoustic energy.

V. CONCLUSIONS

The theoretical analysis developed in this study allows the determination of the temperature difference that occurs at the regenerator interface in open cycle traveling wave thermoacoustic engines, when mean flow replaces the hot heat exchanger as a means for supplying heat to the engine. This temperature difference is shown to be a function of five independent dimensionless parameters, and is well approximated by Eq. (26) above. With slight modifications, the theoretical framework developed in this study could also be used to evaluate open cycle designs for traveling wave thermoacoustic refrigerators and heat pumps. The temperature differences predicted by these analyses could significantly affect the performance of these open cycle devices, and may positively or negatively affect their feasibility as alternatives to their closed cycle counterparts. Previous studies on thermoacoustic temperature differences typically associate them with loss mechanisms, where minimizing them generally improves the performance of the thermoacoustic device. This is not found to be the case in the open cycle thermoacoustic engine, however, since reducing the temperature difference has the direct effect of reducing the acoustic power output of the engine, according to Eq. (28).

Predicting the existence of this temperature difference is the first step in the evaluation of the feasibility of open cycle traveling wave thermoacoustic devices, and suggests several subsequent avenues of research. For instance, the losses that result from the heat transferred across the potentially large temperature difference could be analyzed and compared to the losses in the hot heat exchanger of a closed cycle thermoacoustic engine. Also, the effects of this temperature difference on the theoretical efficiencies of open cycle devices could be studied and compared to those of closed cycle devices. Finally, given the potential for increasing the efficiencies of thermoacoustic devices by employing open cycle configurations, these analyses need to be verified in the laboratory to determine the accuracy of the assumptions and predictions that are made in these studies.

ACKNOWLEDGMENT

The authors would like to thank Greg Swift for his helpful discussion of this topic.

[1] R. S. Reid, W. C. Ward, and G. W. Swift, "Cyclic thermodynamics with open flow," Phys. Rev. Lett. **80**, 4617–4620 (1998).
[2] R. S. Reid and G. W. Swift, "Experiments with a flow-through thermoacoustic refrigerator," J. Acoust. Soc. Am. **108**, 2835–2842 (2000).
[3] R. S. Reid, "Open cycle thermoacoustics," Ph.D. thesis, Georgia Institute of Technology, School of Mechanical Engineering, 1999.
[4] S. Backhaus and G. W. Swift, "A thermoacoustic-Stirling heat engine: Detailed study," J. Acoust. Soc. Am. **107**, 3148–3166 (2000).
[5] J. J. Wollan, G. W. Swift, S. Backhaus, and D. L. Gardner, "Development of a thermoacoustic natural gas liquefier," AIChE Meeting, New Orleans, LA, 11–14 March 2002. Available at: http://www.lanl.gov/thermoacoustics/Pubs/index.html.
[6] J. L. Smith and M. Romm, "Thermodynamic loss at component interfaces in Stirling cycles," Proceedings of the 27th Intersociety Energy Conversion Engineering Conference, San Diego, CA, Society of Automotive Engineers, 1992, pp. 5.529–5.532.
[7] G. W. Swift, "Analysis and performance of a large thermoacoustic engine," J. Acoust. Soc. Am. **92**, 1551–1563 (1992).
[8] J. R. Brewster, R. Raspet, and H. E. Bass, "Temperature discontinuities between elements of thermoacoustic devices," J. Acoust. Soc. Am. **102**, 3355–3360 (1997).
[9] P. Kittel, "The temperature profile within pulse tubes," Adv. Cryog. Eng. **43**, 1927–1932 (1998).
[10] L. Bauwens, "Interface loss in the small amplitude orifice pulse tube model," Adv. Cryog. Eng. **43**, 1933–1940 (1998).
[11] G. W. Swift, *Thermoacoustics: A Unifying Perspective for Some Engines and Refrigerators* (Acoustical Society of America, Melville, NY, 2002).